Quantum-chemical study of the isobutane cracking on zeolites

Please check the document version of this publication:

• A submitted manuscript is the version of the article upon submission and before peer-review. There can be important differences between the submitted version and the official published version of record. People interested in the research are advised to contact the author for the final version of the publication, or visit the DOI to the publisher's website.
• The final author version and the galley proof are versions of the publication after peer review.
• The final published version features the final layout of the paper including the volume, issue and page numbers.
Link to publication

Quantumchemical study of the isobutane cracking on zeolites

V.B. Kazansky [a,*], M.V. Frash [a], R.A. van Santen [b]

[a] *Zelinsky Institute of Organic Chemistry, Russian Academy of Sciences, Moscow B-334, Russian Federation*
[b] *Eindhoven University of Technology, P.O. Box 513, Eindhoven, Netherlands*

Abstract

The ab initio quantumchemical investigation of the elementary steps of the catalytic isobutane cracking is presented. A reasonable agreement between experimental and theoretical activation energies is found. The obtained results demonstrate that the adsorbed carbenium and carbonium ions represent not the really existing reaction intermediates, but the high-energy transition states of the corresponding elementary reactions. This results in much higher activation energies than for the similar reactions in homogeneous super-acid solutions.

Keywords: Alkanes; Carbenium ions; Carbonium ions; Cracking; Isobutane; Isobutene; Transition states

1. Introduction

Catalytic cracking of paraffins on such solid acids as zeolites and amorphous silica–alumina catalysts is widely used by chemical industry for oil refining. It is generally accepted that this is a chain reaction, which involves adsorbed carbenium and carbonium ions as active intermediates [1]. The reaction mechanism is mainly supported by the study of kinetics and by the final reaction products. It usually includes the following main elementary steps:

I. Chain initiation resulting in formation of adsorbed carbenium ions. This can occur according to any of the following elementary reactions:By protonation of olefins:

$$H_{ads}^+ + olefin \rightarrow R_{ads}^+ \tag{1}$$

---

* Corresponding author.

By protolytic cracking of paraffins:

$$H^+_{ads} + RH \rightarrow R_1H + R^+_{2\,ads} \qquad (2)$$

By protolytic dehydrogenation of paraffins:

$$H^+_{ads} + RH \rightarrow H_2 + R^+_{ads} \qquad (3)$$

II. Chain termination, which represents the reverse of the reaction (1):

$$R^+_{ads} \rightarrow H^+_{ads} + olefin \qquad (4)$$

III. Chain propagation which can involve:Hydride transfer:

$$RH + R^+_{1\,ads} \rightarrow R^+_{ads} + R_1H \qquad (5)$$

Skeletal isomerisation of adsorbed carbenium ions:

$$R^+_{ads} \rightarrow i - R^+_{ads} \qquad (6)$$

Cracking of adsorbed carbenium ions:

$$R^+_{ads} \rightarrow R^+_{1\,ads} + olefin \qquad (7)$$

The reverse reaction of carbenium ions with olefins resulting in oligomerisation:

$$R^+_{ads} + olefin \rightarrow R_1H^+_{ads} \qquad (8)$$

Considerable results in the understanding of some details of the above elementary steps have been recently achieved for cracking of light paraffins on zeolites. For these relatively simple molecules one can discriminate between different mechanisms of chain initiation from the distribution of the reaction products at conversions below 1%. Such experiments indicated that at high temperature and low pressure the chain initiation mainly proceeds through direct protonation of light paraffins according to reactions (2) and (3), which involve formation of adsorbed pentacoordinated carbonium ions as active intermediates [2].

For instance, for isobutane cracking on faujasites [3–10] at relatively low conversions the rates of reactions (2) and (3) are comparable, and the chain propagation mainly proceeds by hydride transfer according to reaction (5). This results in the chain length varying within 3–5 depending on the reaction conditions [9]. The apparent activation energies of reactions (2) and (3) of protolytic cracking and dehydrogenation are practically equal to each other (39.6 and 37.5 kcal/mol, respectively) [10]. In Refs. [11,12] a kinetic model of isobutane cracking was worked out, which includes 21 elementary steps. A good fitting of calculated reaction parameters with experimental data was obtained. The initial steps of n-butane and n-pentane cracking were also studied in Refs. [8,13].

Kinetic regularities represent only one source of information concerning the mechanism of cracking. The other possibility consists in quantumchemical analysis of various elementary steps of the reaction. This was, however, done

only in a quite few published papers, which are mainly devoted to the study of adsorbed carbenium ions. For instance, it was concluded in Ref. [14] that these species represent the activated complexes, whereas the real surface intermediates resulting from ethene interaction with bridging hydroxyl groups of zeolites are the covalently bonded alkoxides. The latter species are formed from the surface π-complexes through the carbenium-ion-like transition state, which strongly resembles in geometry and charge distribution the classical ethyl carbenium ion. In Ref. [15] the similar conclusion was made for formation of surface *sec*-propyl and *tert*-butyl fragments.

The adsorbed nonclassical carbonium ions were also a subject of quantum-chemical investigations. In Ref. [16] the conception of carbonium-ion-like transition states was applied to hetero-isotope exchange of CD_4 with protons of zeolites. An attempt to use the "ab initio" quantumchemical calculations for analysis of protolytic cracking and dehydrogenation of ethane according to reactions (2) and (3) was done in Refs. [17,18], and of dehydrogenation of methane in Refs. [18,19]. The corresponding activation energies were found to be very high. This looks, however, quite natural, since cracking and dehydrogenation of ethane are certainly very difficult reactions. Consequently, more realistic models involving higher hydrocarbons should be also discussed. Indeed, the possible pathways of n-butane cracking were speculated in Ref. [20] and analysed by means of semi-empirical calculations in Ref. [21].

The aim of this paper is the "ab initio" quantumchemical study of the nature of adsorbed carbenium and carbonium ions and of their role in the most of the above mentioned elementary steps. This was done for the isobutane cracking on zeolites, which involves the adsorbed *tert*-butyl carbenium and carbonium ions. Both of these species are most often considered as the active intermediates in acid-catalysed transformations of light paraffins.

Below we will discuss the mechanism of chain initiation according to reactions (1), (2) and (3), of the chain termination according to reaction (4), and of the chain propagation via hydride transfer according to reaction (5). On the other hand, the skeletal isomerisation of *tert*-butyl fragment (6) is obviously of no interest. Therefore, among the above elementary steps only reactions (7) and (8) will remain outside the scope of this paper.

2. Models and computational details

The "ab initio" quantumchemical calculations were performed with the GAUSSIAN-92 program [22]. Due to the relatively large size of the hydrocarbon fragments (up to 8 carbon atoms for hydride transfer), the Brønsted acid sites of zeolites were modelled by the simplest $H(OH)Al(OH)_3$ cluster (differences in activation energies calculated with this smallest cluster and larger $H_3Si(OH)AlH_2OSiH_3$ cluster were estimated for small hydrocarbon fragments).

The geometries of the investigated structures were fully optimised at the SCF theory level using the standard 6-31G* basis set [23–25]. The gradient technique [26] was applied for these optimisations. The transition state structures were found by minimising the gradient norm. Analytical frequency calculations were performed in order to verify the nature of the obtained stationary points. In addition, intrinsic reaction coordinate method (IRC) [27] was applied for passing from each transition state to the initial and the final products.

Single point calculations were carried out for the optimised structures, in the frame of second-order Møller-Plesset perturbation theory [28] with a 6-31 + + G** basis set. Corrections for zero-point energy (ZPE) obtained from frequency calculations were included in final activation energies and enthalpies (unscaled frequencies were used). The potential-fitted atomic charges obtained according to the CHELPG scheme [29] at the HF/6-31 + + G**//6-31G* level, were applied for the analysis of the charge distribution in the calculated structures.

Total energies of the investigated structures, zero-point energies and imaginary frequencies for transition states are collected in Table 1.

Below for designation of particular atoms in the structures under discussion we shall use the line numbers (for example C2), whereas the underline numbers will be used for designation of the atomic groups (for example CH$_3$ is a methyl fragment).

3. Results

3.1. Chain initiation by protonation of isobutene

The energy diagram of the isobutene interaction with the surface bridging hydroxyl groups of zeolites reconstructed from the results of our calculations is depicted in Fig. 1a. The geometries of the reaction intermediates and that of the resulting alkoxide groups are presented in Fig. 2. The most important parameters of the corresponding structures are also collected in Table 2.

In accordance with earlier calculations performed for ethene [14,31] and for propene and isobutene [15], the reaction starts with the formation of the π-complex. This elementary step does not require any activation energy and is exothermic at the MP2/6-31 + + G**//6-31G* level (with ZPE corrections) by 7.4 kcal/mol. This is slightly less than the values of 8.2–11 kcal/mol calculated in Ref. [15] with different basis sets. Only minor changes in both cluster and isobutene geometry take place when the π-complex is formed. The positive charging of adsorbed olefin is also quite small (+0.078e). It is mainly connected with electron density transfer to the proton of the bridging hydroxyl, since the positive charge of the latter decreases by 0.082e.

Then the π-complex is transformed into a covalently bonded *tert*-butyl

Table 1
Total energies of investigated structures, zero-point energies and imaginary frequencies (for transition states)

Structure	Total energy (au)		Zero-point energy (kcal/mol)	Imaginary frequency (cm^{-1})
	HF/6-31G*	MP2/6-31++G**//6-31G$^+$	HF/6-31G*	HF/6-31G*
H$_2$	-1.1268278	-1.1577576	6.6	–
CH$_4$	-40.1951719	-40.3660952	30.0	–
C$_3$H$_8$	-118.2636512	-118.7297107	69.4	–
i-C$_4$H$_8$	-156.1106670	-156.6998814	72.6	–
i-C$_4$H$_{10}$	-157.2989780	-157.9162823	88.3	–
Free cluster H(OH)Al(OH)$_3$	-544.4434665	-545.3274352	44.7	–
π-complex	-700.5634785	-702.0407458	118.3	–
Surface propoxide sec-C$_3$H$_7$–(OH)Al(OH)$_3$	-661.5515388	-662.8735209	101.8	–
Surface butoxide tert-C$_4$H$_9$–(OH)Al(OH)$_3$	-700.5898876	-702.0656787	120.5	–
TS-I (for i-butene protonation)	-700.5120325	-701.9987521	114.6	-1084
TS-II (for i-butane cracking)	-701.6196652	-703.1492160	131.2	-432
TS-III (for i-butane dehydrogenation)	-701.6146104	-703.1279360	127.1	-537
TS-IV (for i-butane dehydrogenation with direct formation of i-butene [a]	-701.6038705	-703.1153746	127.2	-307
				-44
				-17
TS-V (for hydride transfer)	-857.7737704	-859.8989034	205.2	-423

[a] The partial geometry optimisation for this transition state (see Section 3.4) caused three imaginary frequencies instead of one. Relaxation at both sides of the top of barrier was applied for testing of this transition state instead of IRC analysis.
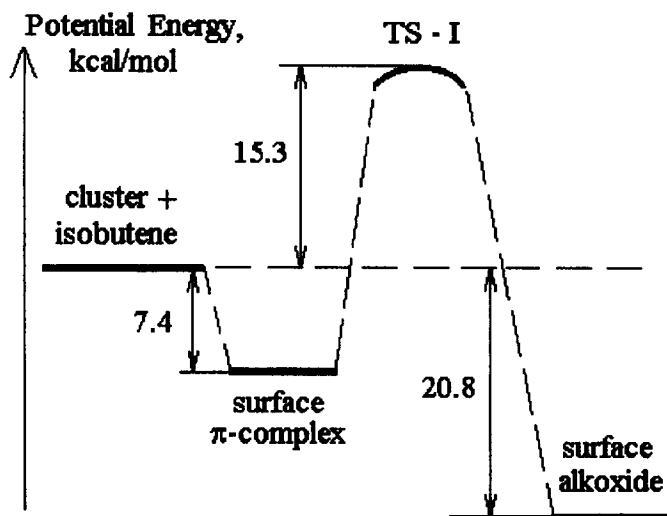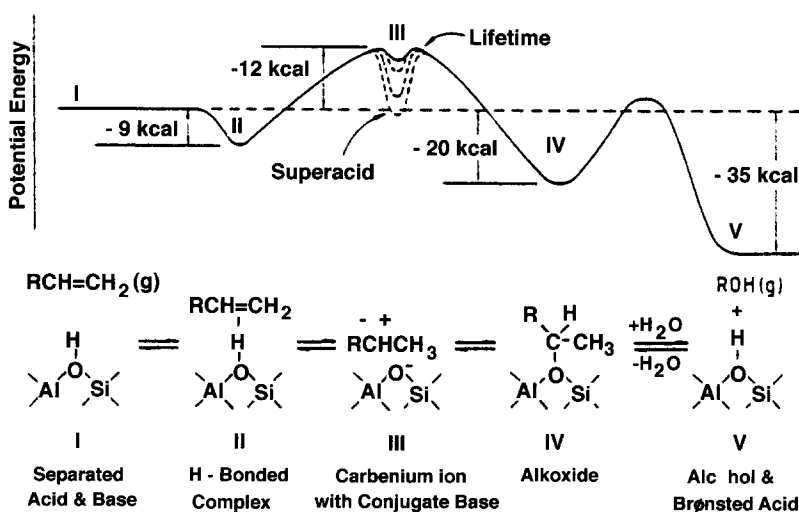
Fig. 1. Energy profile for protonation of isobutene. (a) Results of our calculations. (b) Estimations of Engelhardt and Hall. Reproduced with permission from Ref. [30], Copyright 1995 Academic Press, Inc.

group. The conclusion about the covalent nature of the C–O bond in this most stable final structure follows from the short C–O distance of 1.458 Å, from the geometry of *tert*-butyl fragment with near-tetrahedral (close to 109°) angles at the tertiary carbon atom, and from an only moderate positive charge of the alkyl
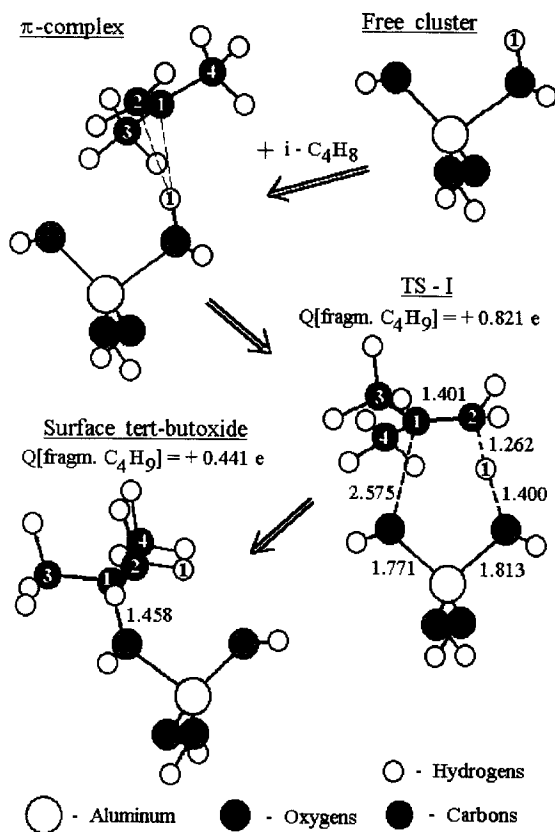
Fig. 2. Protonation of isobutene.

group of +0.441e. The reaction is exothermic by 13.4 kcal/mol. This is close to the heat effects of 7.3–11.3 kcal/mol obtained from quantumchemical calculations in Ref. [15].

The transformation of the π-complex into a covalently bonded surface *tert*-butyl fragment occurs through a transition state TS-I of Fig. 2 with an activation energy of 22.7 kcal/mol. This is somewhat less than the value of 30.1 kcal/mol obtained from quantumchemical calculations in Ref. [15]. The difference is most likely accounted for different basis sets and cluster dimensions used in Ref. [15] and in our work.

The general features of the π-complex transformation into alkoxide are in full agreement with earlier calculations [14,15,31]. Indeed, the geometry of the TS-I transition state of Fig. 2 resembles that of the classical *tert*-butyl carbenium ion. This follows from the much higher positive charge of the *tert*-butyl fragment of +0.821e than that of the covalently bonded alkoxide (+0.441e). In addition, the C_4H_9 group becomes almost flat as it should be expected for a classical *tert*-butyl carbenium ion (the sum of angles C2–C1–C3, C2–C1–C4, and

Table 2

Relevant HF/6-31G* geometrical parameters and atomic charges for free cluster, isobutene, π-complex, transition state for isobutene protonation, and surface tert-butoxide

	Free cluster	Isobutene	π-complex	TS-1	Surface tert-butoxide
d(Al–O1)	1.979	–	1.958	1.813	1.722
d(Al–O2)	1.720	–	1.723	1.771	1.946
d(O1–H1)	0.954	–	0.961	1.400	2.655
d(H1–C1)	–	–	2.519		
d(H1–C2)	–	–	2.311	1.262	1.082
d(O2–C1)	–	–	4.091	2.575	1.458
d(C1–C2)	–	1.321	1.328	1.401	1.524
$\angle$Al–O1–H1	106.4	–	115.3	109.5	–
$\angle$C2–C1–C3	–	122.3	122.3	120.2	111.9
$\angle$C2–C1–C4	–	122.3	122.0	120.5	111.6
$\angle$C3–C1–C4	–	115.4	115.7	118.7	112.3
q(O1)	–0.735	–	–0.723	–1.021	–1.019
q(O2)	–1.054	–	–1.039	–1.021	–0.664
q(H1)	+0.460	–	+0.378	+0.480	+0.118
q(C1)	–	+0.245	+0.330	+0.749	+0.709
q(C2)	–	–0.669	–0.641	–0.707	–0.329
q(fragm. C_4H_8)	–	0.0	+0.078	–	–
q(fragm. C_4H_9)	–	–	–	+0.821	+0.441

Distances in Å; angles in deg; potential-fitted (according to the CHELPG scheme at the HF/6-31 + + G**//6-31G* level) charges in units of electron charge.

C3–C1–C4 is almost equal to 360°). Finally, the C–O bond in the transition state (2.575 Å) is considerably longer than in the covalently bonded alkoxide (1.458 Å).

The cyclic structure of such a transition state indicates the bifunctional nature of the active site. Indeed, its Brønsted acid part protonates the adsorbed olefin, whereas the interaction with the neighbouring basic oxygen converts the protonated hydrocarbon into the final surface alkoxide. This is assisted by the "switching" of the Al–O bonds of the cluster, which are almost equally long in the transition state, but considerably differ from each other in the initial and the final structures (in both cases the Al–O bond with three-coordinated oxygen is longer).

The energy diagram of Fig. 1a very much resembles the one of Fig. 1b which was recently discussed for the interaction of olefins with surface OH groups of zeolites by Engelhardt and Hall in Ref. [30]. Indeed, in both cases the reaction follows the same sequence of elementary steps with close values of heat effects or activation energies: olefin → π-complex (heat effects of 7.4 or 9 kcal/mol respectively); π-complex → surface alkoxide (heat effects of formation from olefin and the hydroxyl group are equal to 20.8 and 20 kcal/mol with activation energies of 15.3 and 12 kcal/mol respectively).

On the other hand, both these schemes strongly differ in the interpretation of the nature of the adsorbed carbenium ions. According to our and other previous

quantumchemical calculations these species represent the transition states, whereas Engelhardt and Hall consider them as metastable reaction intermediates with a lifetime which is dependent on the acid strength of the OH groups from which these species were formed (the stronger are the OH groups the longer is the lifetime of such carbenium ions and the more chemically active they are).

The former conception is certainly more realistic than the traditional interpretation of the adsorbed carbenium ions as really existing reaction intermediates, when the difference between these ionic species and the surface alkoxides is even not considered and the role of π-complexes in the formation of carbenium ions is even not discussed. On the other hand, the quantumchemical approach certainly makes the next step in the understanding of the real mechanism of the carbenium ion reactions, since it provides information on the geometry of carbenium-ion-like transition states and on the nature of their interaction with the surface. The results of calculations also present a reasonable estimation both of the heats and activation energies of the elementary steps with participation of these species.

3.2. Chain termination

The chain termination according to reaction (4) represents the decomposition of the *tert*-butoxide group into isobutene and bridging hydroxyl. This is the reverse of Eq. (1). The reaction coordinate mainly involves the stretching of the C–O bond, which makes it more polar and the *tert*-butyl fragment more positively charged. Simultaneously the alkyl group declines toward the neighbouring oxygen of the cluster due to hydrogen bonding of one of the methyl groups with this basic site. On the top of the activation barrier the hydrogen bond is the strongest, whereas the positive charge of the *tert*-butyl fragment is the highest. This is the same "carbenium-ion-like" transition state as that one already discussed in the previous paragraph. The calculated activation energy of the *tert*-butyl alkoxide decomposition into isobutene and the bridging hydroxyl is equal to 36.1 kcal/mol. This is in good agreement both with the value of 36.84 kcal/mol, which was used for modelling of isobutane cracking in Refs. [10–12], and with that of 41.4 kcal/mol obtained from the quantumchemical calculations in Ref. [15].

3.3. Protolytic cracking

This reaction is found to be similar to protolytic cracking of ethane [17], since it starts with a proton attack at the C–C bond of isobutane. The C_4H_{11} fragment in the transition state TS-II of Fig. 3 (see also Table 3) is oriented almost perpendicularly to the O1–Al–O2 plane. By the high total positive charge of +0.909e and geometry it very much resembles a nonclassical $C_4H_{11}^+$ carbonium ion, where the isopropyl and the methyl groups are connected with each other by
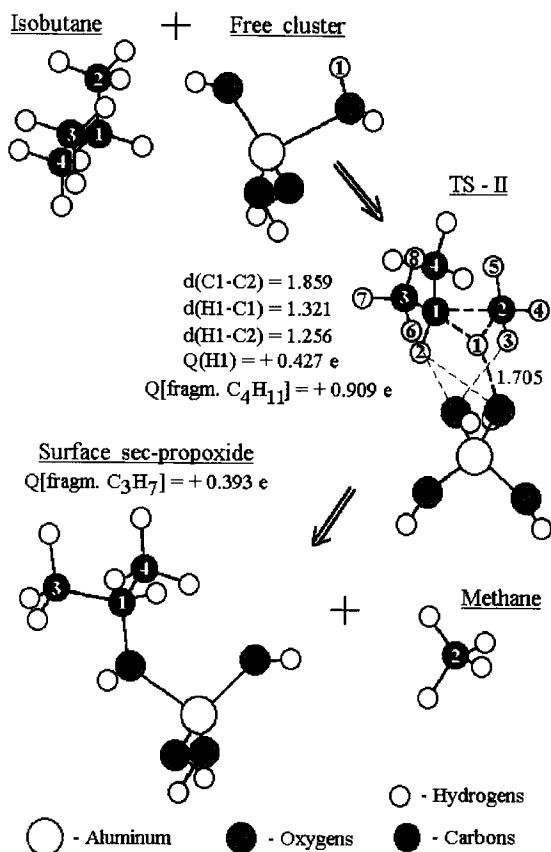
d(C1-C2) = 1.859
d(H1-C1) = 1.321
d(H1-C2) = 1.256
Q(H1) = + 0.427 e
Q[fragm. C_4H_{11}] = + 0.909 e

Surface sec-propoxide
Q[fragm. C_3H_7] = + 0.393 e

○ - Hydrogens

○ - Aluminum   ● - Oxygens   ● - Carbons

Fig. 3. Protolytic cracking of isobutane.

Table 3
Relevant HF/6-31G* geometrical parameters and atomic charges for free cluster, isobutane, transition state for isobutane cracking, and surface sec-propoxide

	Free cluster	Isobutane	TS-II	Surface sec-propoxide
d(O1–H1)	0.954	–	1.705	–
d(O2–C1)	–	–	3.242	1.447
d(H1–C1)	–	–	1.321	–
d(H1–C2)	–	–	1.256	–
d(C1–C2)	–	1.531	1.859	–
∡C1–H1–C2	–	–	92.3	–
∡(C1–C2)–(O1AlO2)	–	–	86.4	–
q(H1)	+ 0.460	–	+ 0.427	–
q(C1)	–	+ 0.532	+ 0.233	+ 0.504
q(C2)	–	– 0.301	– 0.351	–
q(fragm. CH_3)	–	– 0.143	+ 0.153	–
q(fragm. C_3H_7)	–	+ 0.143	+ 0.329	+ 0.393
q(fragm. C_4H_{11})	–	–	+ 0.909	–

Distances in Å; angles in deg; potential-fitted (according to the CHELPG scheme at the HF/6-31 + + G**//6-31G* level) charges in units of electron charge.
Values for CH_4: d(C–H) = 1.084; q(C) = – 0.340; q(H) = + 0.085.

the hydrogen atom (the most important HF/6-31G* geometry parameters of the free carbonium ion are: d(C1–C2) = 3.546 Å; d(C1–H1) = 3.234 Å; d(C2–H1) = 1.086 Å, $\angle$C1–H1–C2 = 94.4°). One can also distinguish a strongly perturbed positively charged methane-like fragment (Q(CH$_4$) = +0.580e) with the stretched by 0.172 Å C2–H1 bond, that is formed in the reaction.

On the other hand, due to the hydrogen bonding of the bridging H1 atom with the O1 basic oxygen of the cluster (d(O1–H1) = 1.705 Å), the adsorbed carbocation has a high positive charge on this hydrogen atom of +0.427e (the charge of the bridging hydrogen atom in the free carbocation (sec-C$_3$H$_7$–H–CH$_3^+$), calculated according to the CHELPG scheme at the HF/6-31 + + G**//6-31G* level, is equal to +0.056e). Relatively weaker hydrogen bonds with the surface oxygens are also formed by the three other hydrogens (H2, H3 and H6 in Fig. 3). This results in polarisation of corresponding C–H bonds. Therefore, the positive charge of the H3 hydrogen of the methyl group directed towards the surface of +0.211e is somewhat higher than those of the H4 (+0.146e) and H5 (+0.147e) hydrogens directed from the surface. Similarly, the positive charge of the H6 hydrogen directed towards the surface (+0.102e) is higher than that of the H7 (+0.084e) and H8 (+0.065e) hydrogens. This also indicates the polarisation of the hydrocarbon fragment due to interaction with the surface.

The decomposition of this transition state occurs by abstraction of methane and by the approach of the isopropyl fragment to the basic O2 oxygen of the cluster. This results in the surface sec-propyl alkoxide and similar to reactions (1) and (4) demonstrates the bifunctional Brønsted acidic–Lewis basic nature of the active site.

The reaction of protolytic cracking of isobutane is practically thermoneutral with an activation energy of 57.5 kcal/mol. This is much lower than the earlier reported [17] value for cracking of ethane of 93.4 kcal/mol obtained with the 3-21G basis set and with only partial geometry optimisation. Therefore, we reproduced our previous calculations for ethane at the MP2/6-31 + + G**//HF/6-31G* level with full geometry optimisation. In this case the activation energy for ethane cracking was found equal to 80.3 kcal/mol. This is still much higher than for isobutane cracking, and should be explained by the more difficult formation of the adsorbed methylcarbenium-ion-like fragment in comparison with the sec-C$_3$H$_7^+$ carbocation.

3.4. Dehydrogenation

The reaction path for protolytic dehydrogenation is depicted in Fig. 4 (see also Table 4). The geometry of the TS-III transition state for this reaction is quite different from the previous ones. It rather indicates a protolytic attack at the H2 hydrogen atom of the isobutane than at the C1–H2 bond. The resulting activated complex resembles a polarised hydrogen molecule placed between the
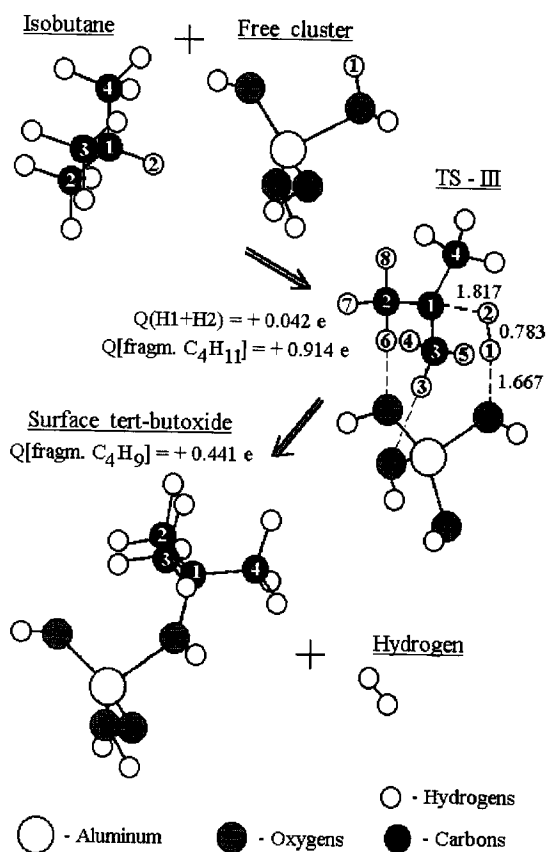
Fig. 4. Protolytic dehydrogenation of isobutane.

Table 4

Relevant HF/6-31G* geometrical parameters and atomic charges for free cluster, isobutane, transition state for isobutane dehydrogenation, and surface *tert*-butoxide

	Free cluster	Isobutane	TS-III	Surface *tert*-butoxide
d(O1–H1)	0.954	–	1.667	–
d(O1–C1)	–	–	3.432	1.458
d(H1–H2)	–	–	0.783	–
d(C1–H2)	–	1.089	1.817	–
d(C1–H1)	–	–	2.216	–
$\angle$(C1–H1)–(O1AlO2)	–	–	70.9	–
q(H1)	+ 0.460	–	+ 0.231	–
q(H2)	–	− 0.109	− 0.187	–
q(C1)	–	+ 0.532	+ 0.759	+ 0.709
q(fragm. C_4H_9)	–	+ 0.109	+ 0.872	+ 0.441
q(fragm. C_4H_{11})	–	–	+ 0.914	–

Distances in Å; angles in deg; potential-fitted (according to the CHELPG scheme at the HF/6-31 + + G**//6-31G* level) charges in units of electron charge.
Value for H_2: d(H–H) = 0.730.

tert-butyl carbenium ion and the negatively charged cluster. Indeed, the H1 atom has a positive charge $+0.231e$, whereas the H2 atom is charged negatively $(Q(H2) = -0.189e)$. This results only in a small total charging of the abstracting H_2 fragment ($+0.042e$), and in an only slightly longer (by 0.053 Å) H1–H2 distance with respect to the free hydrogen molecule. At the same time, the *tert*-butyl group in such a transition state has a very high positive charge of $+0.872e$. The protolytic dehydrogenation is endothermic by 6.9 kcal/mol.

The intrinsic reaction coordinate analysis [27] shows that after abstraction of the hydrogen molecule, the *tert*-butyl group moves to the O1 oxygen atom, i.e. to the same oxygen which was connected in the initial cluster with the acidic proton. Consequently, protolytic dehydrogenation could not be considered as a concerted reaction. On the other hand, the hydrogen bonds of a hydrocarbon fragment with basic O2 and O3 oxygen atoms of the cluster ($d(O2–H6) = 2.109$ Å; $d(O3–H3) = 2.163$ Å) are quite important for the geometry of this transition state. Therefore, as in the case of transition state for protolytic cracking, the hydrogen atoms directed towards the surface have somewhat higher positive charges than other hydrogens. For example, the H3 hydrogen has a charge of $+0.266e$, whereas that of the connected to the same C2 carbon H4 and H5 hydrogens are only $+0.127$ and $+0.123e$, respectively.

One can rationalise the difference between the transition states of dehydrogenation and cracking in the following way. In case of dehydrogenation the proton attack results in polarisation of the C1–H2 bond with a displacement of electronic density from the carbon towards the hydrogen atom. This is in contradiction with electronegativities of these atoms. In addition, in the transition state of dehydrogenation the positively charged central carbon atom of the *tert*-butyl fragment is rather far from the negatively charged active site due to the steric repulsion of three methyl groups, whereas the *sec*-propyl fragment in the transition state for cracking is closer to the cluster. The two latter factors are unfavourable for dehydrogenation with respect to cracking. As a consequence we obtained an activation energy for dehydrogenation of 66.8 kcal/mol, which is considerably higher than that obtained for cracking of 57.5 kcal/mol.

On the other hand, the comparison of these figures with the published experimental values indicates, however, some discrepancy since in Ref. [10] the activation energies for cracking and dehydrogenation were found almost equal. Therefore, we performed a search of alternative pathways for the dehydrogenation reaction.

At first, we have found a transition state, which is similar to TS-III, but with two hydrogen bonds with the same oxygen atom O2. The corresponding activation energy was, however, only by 0.7 kcal/mol higher than for the pathway discussed above. This difference is practically insignificant. Therefore, we shall not specially discuss this pathway.

We also considered a direct isobutane dehydrogenation resulting in isobutene and free surface hydroxyl instead of surface *tert*-butoxide. The corresponding
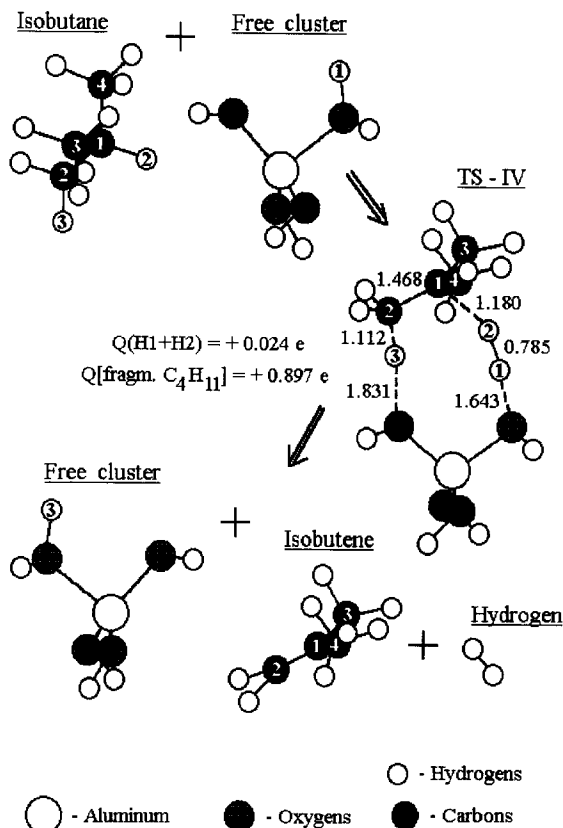
Fig. 5. Protolytic dehydrogenation of isobutane with direct formation of isobutene.

Table 5

Relevant HF/6-31G* geometrical parameters and atomic charges for free cluster, isobutane, transition state for isobutane dehydrogenation with direct formation of isobutene, and isobutene

	Free cluster	Isobutane	TS-IV	Isobutene
d(O1–H1)	0.954	–	1.643	–
d(H1–H2)	–	–	0.785	–
d(H2–C1)	–	1.089	1.180	–
d(C1–C2)	–	1.531	1.468	1.321
d(C2–H3)	–	1.087	1.112	–
d(O2–H3)	–	–	1.831	–
q(H1)	+0.460	–	+0.359	–
q(H2)	–	−0.109	−0.335	–
q(C1)	–	+0.531	+0.710	+0.245
q(C2)	–	−0.301	−0.437	−0.669
q(H3)	–	+0.054	+0.318	–
q(fragm. C_4H_{11})	–	–	+0.897	–

Distances in Å; angles in deg; potential-fitted (according to the CHELPG scheme at the HF/6-31 + + G**//6-31G* level) charges in units of electron charge.

TS-IV is depicted in Fig. 5 (see also Table 5). It represents a concerted reaction. Indeed, the acidic H1 hydrogen of the cluster abstracts the H2 hydrogen atom from the isobutane molecule as a "hydride ion" (the charge on this atom in the transition state is −0.335). Simultaneously the H3 hydrogen atom moves as a "proton" towards the O2 oxygen. The zeolite surface does not change during this elementary reaction and only acts as a "conductor" of the proton.

One should, however, note that unlike the other transition states, the TS-IV was found with some geometry restrictions. Namely, two carbon atoms C1 and C2 were kept in the O1–Al–O2 plane. This resulted in 3 imaginary frequencies instead of one for other transition states. An attempt to release all degrees of freedom resulted in rearrangement of this transition state into the discussed above TS-III.

The activation energy of direct dehydrogenation is equal to 74.7 kcal/mol, being by 7.9 kcal/mol higher than for the above discussed pathway resulting in the surface tert-butoxide. Consequently, the latter pathway appears to be the optimum among the above investigated protolytic dehydrogenation reactions.

Such a pathway of isobutane dehydrogenation is similar to the one previously discussed for dehydrogenation of ethane and methane in Refs. [18,19]. On the other hand, the activation energy of 66.8 kcal/mol for isobutane dehydrogenation is much lower than that of 94.8 kcal/mol previously obtained in Ref. [18] with the 3-21G basis set and only partial geometry optimisation. Therefore, we reproduced the previous calculations for ethane dehydrogenation at the MP2/6-31 + + G **//HF/6-31G * level with full geometry optimisation. The obtained value of 83.8 kcal/mol makes the difference in activation energies for ethane and isobutane dehydrogenation more reasonable.

3.5. Hydride transfer

Unlike protolytic cracking or dehydrogenation, hydride transfer is a secondary reaction. Therefore, the experimental study of this elementary step is more difficult and direct data concerning the activation energy of the hydride transfer with participation of surface tert-butoxides are absent. The only available estimation of this value of about 30 kcal/mol was made in the papers on modelling of isobutane cracking [11,12]. There are also some indications that the activation barrier of the hydride transfer should be somewhat lower than for dehydrogenation or cracking , i.e. less than 40 kcal/mol [10].

Below the hydride transfer was studied for the degenerated reaction between surface tert-butoxide and isobutane:

$$t\text{-}C_4H_{9\,surf}^+ + i\text{-}C_4H_{10} \rightarrow i\text{-}C_4H_{10} + t\text{-}C_4H_{9\,surf}^+ \tag{5a}$$
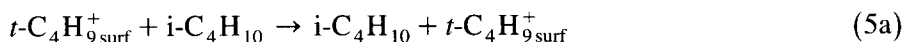
The reaction starts with the isobutane attack at the C–O bond of the covalently bonded tert-butyl alkoxide. This results in a considerable increase of the C–O distance and in the change of the tert-butyl group orientation relative
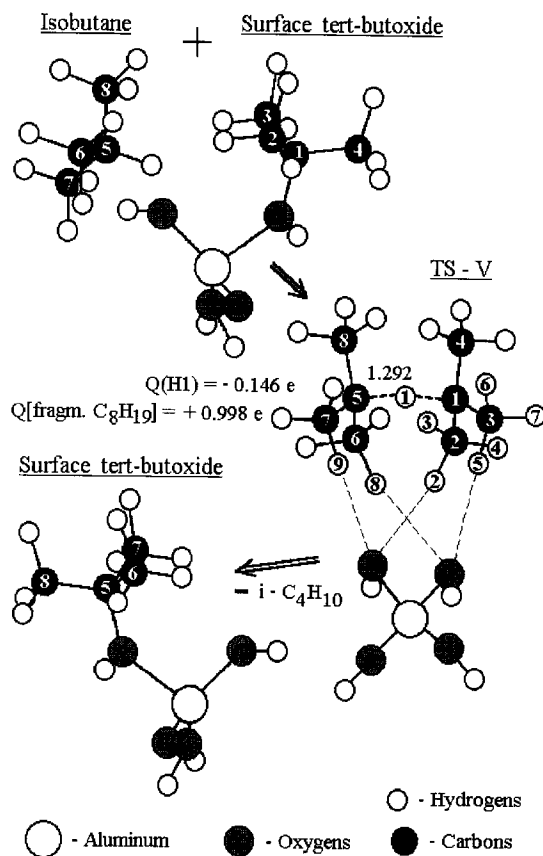
Fig. 6. Hydride transfer from isobutane to surface *tert*-butoxide.

Table 6

Relevant HF/6-31G* geometrical parameters and atomic charges for surface *tert*-butoxide, isobutane, and transition state for hydride transfer

	Surface *tert*-butoxide	Isobutane	TS-V
d(O2–C1)	1.458	–	3.809
d(C1–H1) = d(C5–H1)	–	1.089	1.292
$\angle$C1–H1–C5	–	–	179.8
$\angle$(C1–C5)–(O1AlO2)	–	–	68.8
q(H1)	–	−0.109	−0.146
q(C1) = q(C5)	+0.709	+0.532	+0.646
q(fragm. C_4H_9)	+0.411	+0.109	+0.572
q(fragm. C_8H_{19})	–	–	+0.998

Distances in Å; angles in deg; potential-fitted (according to the CHELPG scheme at the HF/6-31 + + G**//6-31G* level) charges in units of electron charge.

to the active site in such a way that two of its methyl groups form hydrogen bonds with O1 and O2 oxygen atoms of the cluster (Fig. 6, Table 6). Such a perturbation is much stronger than in the course of *tert*-butyl alkoxide formation

or decomposition according to reactions (1) and (4), since the total positive charge of the hydrocarbon fragment is very high (+0.998e). In other words, the *tert*-butyl group becomes even more "carbenium-ion-like" than in the transition state of the surface alkoxide formation or decomposition. On the other hand, due to the different orientation relative to the cluster, the resulting unstable carbenium ion instead of being adsorbed by the neighbouring basic oxygen abstracts the hydride ion from the attacking isobutane molecule. This results in a symmetric (symmetry C_2) transition state TS-V depicted in Fig. 6.

The geometry and charge distribution in the hydrocarbon fragment of such an activated complex also very much resemble those of the nonclassical carbonium ion resulting from protonation of the central C–C bond in hexamethylethane. The positive charge is equally distributed between both *tert*-butyl fragments, whereas the charge of the hydrogen atom which links these groups is slightly negative (−0.146e). The hydride nature of this bridging hydrogen is also evident from the longer C–H bond of 1.292 Å in comparison with the normal C–H bond length of 1.089 Å.

Four hydrogen atoms in such transition state (H2, H5, H11 and H14) form weak hydrogen bonds with surface O1 and O2 oxygens (d(O1–H2) = d(O2–H11) = 2.162 Å; d(O1–H5) = d(O2–H14) = 2.297 Å). This interaction determines the geometry of the transition state and results in higher positive charges of hydrogen atoms involved in the hydrogen bonds. For example, q(H2) = +0.170e, while q(H3) = +0.091e and q(H4) = +0.068e.

Thus, despite the TS-V transition state for the hydride transfer similar to the TS-II transition state for the isobutane cracking arises from the protonation of the C–C bond of an alkane and also has a very high positive charge on the hydrocarbon fragment, both hydrocarbon fragments quite differently interact with the zeolite surface. Indeed, in TS-II the H1 hydrogen atom has a high positive charge and strongly interacts with an oxygen atom of the surface. On the contrary, in TS-V the H1 hydrogen atom has a negative charge and, therefore, practically does not interact with the surface. This results in different pathways of decomposition of these activated complexes: the first one involves a proton transfer between the cluster and the hydrocarbon, whereas the second one the intermolecular transfer of a hydride-like hydrogen atom.

The calculated activation energy of hydride transfer is equal to 48.4 kcal/mol. This is considerably higher than the value of about 30 kcal/mol used for modelling of isobutane cracking in Ref. [11]. One has, however, to bear in mind that the latter model implied some very rough assumptions.

4. Discussion

The comparison of our results with available literature data is given in Table 7. The main disagreement consists in the somewhat higher values of the

Table 7
A comparison of calculated at MP2/6-31++G**//HF/6-31G* (including corrections for zero-point energies) heat effects (ΔH, kcal/mol) and activation energies ($E\#$, kcal/mol) with available literature data

Reaction	Parameter	Our results	Data from references			Experiments at low conversions [10]
			Calculations [15]	Evaluations [31]	Kinetic model [11,12]	
1 (i-butene protonation)	ΔH_{form} of π-complex [a]	−7.4	−11.0	~−9	–	–
	$E\#$ [a]	15.3	19.1	~12	0	–
	ΔH [a]	−20.8	−22.3	~−20	−36.8	–
2 (cracking)	$E\#$	57.5	–	–	38.1	39.6
	ΔH	1.3	–	–	−2.4	–
3 (dehydrogenation)	$E\#$	66.8	–	–	38.9	37.5
	ΔH	6.9	–	–	−7.6	–
4 (chain termination)	$E\#$	36.1	41.4	~32	36.8	–
	ΔH	20.8	22.3	~20	36.8	–
5 (hydride transfer)	$E\#$	48.4	–	–	~30	< 40

[a] From free i-butene.

calculated activation energies of protolytic cracking (2), dehydrogenation (3) and hydride transfer (5) in comparison with those experimentally measured in Ref. [10] or obtained from modelling of kinetics in Ref. [11]. However, one has to bear in mind, that for protolytic cracking and dehydrogenation the experimentally measured values are the apparent activation energies. Therefore, they should be increased for the heat of isobutane adsorption of about 12–14 kcal/mol [32,33]. In addition, the smallest $H(OH)Al(OH)_3$ cluster used in our calculations has the lower acidity than the real zeolite. Therefore, we tested the influence of the increase of the cluster dimensions on the activation energies of the above three reactions. This was done for the simplest model cases of ethane protolytic cracking, ethane protolytic dehydrogenation and for hydride transfer from methane to surface methoxide (see Table 8). The data of this table show that at the $MP2/6-31 + + G^{**}//HF/6-31G^*$ level the activation energies calculated with the larger $H_3Si(OH)AlH_2OSiH_3$ cluster are by 4–5 kcal/mol lower than with the smallest $H(OH)Al(OH)_3$ cluster. At the $HF/6-31G^*//HF/6-31G^*$ level this difference is even larger (6–9 kcal/mol). It is clear that one can expect a similar decrease of activation energies for transformations of isobutane as well.

The account of both these corrections makes the discrepancy between calculated and experimental values quite small. Thus, the "ab initio" cluster quantumchemical calculations reasonably describe the activation energies and heat effects of the main elementary steps of isobutane cracking.

However, it is even more significant that our results provide a much better understanding of the real nature of adsorbed carbenium and carbonium ions and of their role in some elementary steps of cracking than the classical approach. This circumstance is particularly important, since even in the very recent publications the carbenium ions are still considered as really existing relatively stable intermediates. For instance, when modelling the kinetics of isobutane cracking in Ref. [11], they were not even discriminated from the covalently bonded surface alkoxides. Therefore, the steady state coverage of active sites by adsorbed tert-butyl carbenium ions was estimated as high as 30%!

Only quite recently it was demonstrated that the real stable intermediates in the heterogeneous acid-catalysed transformations of hydrocarbons on zeolites are the covalently bonded alkoxides or surface esters (see Refs. [34,35] and references therein). These species are the precursors of adsorbed carbenium ions, which are formed by partial dissociation or stretching of C–O bonds in the surface esters. Similar to the above discussed mechanism of the chain termination according to reaction (4) this results in separation of charges and in formation of transition states with "carbenium-ion-like" alkyl fragments.

Initially this conclusion was based on the IR study of proton transfer from surface Brønsted acid sites to adsorbed hydrocarbons [34]. Later it was also confirmed by quantumchemical calculations [14,15,31] and more recently by the ^{13}C MAS NMR measurements [36,37]. The above results provide further

Table 8
Effect of cluster size and theory level on the deprotonation energy of cluster and calculated activation energies of the model reactions of ethane protolytic cracking, ethane protolytic dehydrogenation, and hydride transfer from methane to surface methoxide (energies in kcal/mol)

Cluster	H(OH)AlH$_2$(OH) [a]	H(OH)Al(OH)$_3$ [b]		H$_3$Si(OH)AlH$_2$(OSiH$_3$) [b]	
Level of geometry optimisation	HF/3-21G partial optimisation	HF/6-31G* full optimisation		HF/6-31G* full optimisation	
Level of energy calculation	HF/3-21G	HF/6-31G*	MP2/6-31++G** [c]	HF/6-31G*	MP2/6-31++G** [c]
Reaction					
Deprotonation of the cluster	351.9	335.4	317.5	312.5	302.3
Ethane protolytic cracking	93.4	91.3	80.3	82.7	75.4
Ethane protolytic dehydrogenation	94.8	94.4	83.8	88.0	79.5
Hydride transfer from methane to surface methoxide	–	81.9	66.5	72.7	61.3

[a] Data from Refs. [17,18].
[b] Data to be published.
[c] Including corrections for zero-point energy.

convincing evidences supporting these idea. The quantumchemical calculations also confirm that even in the case of the *tert*-butyl carbenium ion the ion pair represents not the short lived metastable complex as was postulated in Ref. [30], but the real transition state [34,38]. Therefore, the different reactivity of adsorbed species depends not on their lifetime on the surface, but on the height of the activation barrier connected with formation of corresponding transition states.

Together with previous publications [17–19], the present paper gives also a much better understanding of the real nature of adsorbed nonclassical carbonium ions. These species also are high-energy transition states resulting from the proton attack at C–C or C–H bonds of paraffins according to reactions (2) and (3) or arising from interaction of paraffins with perturbed surface alkoxides as in the case of hydride transfer (5). The geometry and charge distribution in such "carbonium-ion-like" transition states even in more extent resemble those of the corresponding free ions and their formation requires even higher activation energies than for the "carbenium-ion-like" transition states resulting from protonation of alkenes.

It is very important that, neither the adsorbed carbenium ions, nor the adsorbed carbonium ions could be considered as free species, since they are strongly electrostatically bonded with the surface. For instance, according to our estimation, the abstraction of the *tert*-butyl carbenium ion from the top of the activation barrier in reaction (4) requires an additional energy of about 4 eV. Close electrostatic interaction energies were estimated for adsorbed carbonium ions involved in the transition states of the reactions (2), (3) and (5).

Such a strong Coulomb interaction substantially modifies the geometry and the reactivity of adsorbed species. For instance, it explains the perpendicular orientation of the positively charged hydrocarbon fragments towards the O1–Al–O2 plane of the cluster in transition states TS-II of cracking or in TS-V of the hydride transfer as due to diminishing of steric hindrances and to the more efficient interaction of positive and negative charges. At the same time, both these transition states arising from protonation of the C–C bond, strongly differ from each other due to different type of interaction of the hydrocarbon fragment with the surface. Indeed, in TS-II the H1 hydrogen atom interacts with surface oxygen and the reaction coordinate corresponds to the proton transfer from the surface hydroxyl group to the hydrocarbon. Unlike this, in TS-V the hydrogen atom H1 does not interact with the surface and is transferred from the approaching hydrocarbon molecule moves as a "hydride ion" to the surface hydrocarbon fragment.

It is also very important that both the above calculated activation energies and those experimentally measured for the high temperature transformations of paraffins on zeolites are considerably higher than those obtained for the similar reactions in super-acid solutions [39]. Indeed, the activation energies for protolytic cracking of neopentane with formation of methane and *tert*-butyl cation

in an HF-SbF$_5$ solution is equal to 21 kcal/mol [40] and only to 14 kcal/mol in an HSO$_3$F–SbF$_5$ solution [41]. The activation energy of protolytic dehydrogenation of isobutane in the HF–SbF$_5$ system reported in Ref. [42] is equal to 18.3 kcal/mol, whereas for hydride transfer from isobutane to the *tert*-butyl cation in a SO$_2$–CH$_2$Cl$_2$–AsF$_5$ solution only to 3.6 kcal/mol [43]. All these figures are much lower than for the high temperature reactions on zeolites.

This difference should be accounted for the strong Coulomb interaction of adsorbed species with the surface resulting in considerably higher activation energies in heterogeneous catalytic reactions than in liquid super-acids. Thus, the commonly used mechanism, when the reactions of adsorbed carbenium and carbonium ions are considered in a similar way as those for free carbocations is certainly a very crude simplification.

5. Conclusions

The "ab initio" quantumchemical calculations performed for cracking of isobutane resulted in reasonable values of heat effects and activation energies of the main elementary steps of this reaction. The calculations also demonstrated that both the adsorbed *tert*-butyl carbenium ions and isobutyl carbonium ions represent not the reaction intermediates, but the transition states of corresponding elementary reactions. Although the geometry and charge distribution in such activated complexes very much resemble those of free carbocations, the adsorbed species are strongly held at the active sites by Coulomb interactions. This results in different structures of the transition states for different elementary reactions and modifies the reactivity of the adsorbed species in comparison with free carbocations.

Acknowledgements

References

[1] B.W. Wojcechowski and A. Corma, Catalytic Cracking: Catalysts, Chemistry and Kinetics, Marcel Dekker, New York, 1986.
[2] W.O. Haag and R.M. Dessau, in Proc. 8th Int. Congr. on Catalysis, Berlin 1984, Vol. 2, Dechema, Frankfurt-am-Main, 1984, p. 305.
[3] Mc. Vicker, G.M. Kramer and J.J. Ziemiak, J. Catal., 83 (1983) 286.
[4] E.L. Lombardo and W.K. Hall, J. Catal., 112 (1988) 565.

[5] B. Umansky, J. Engelhardt and W.K. Hall, J. Catal., 127 (1991) 128.
[6] R. Shigeishi, A. Garforth, I. Harris and J. Dwyer, J. Catal., 130 (1991) 423.
[7] C. Stefanadis, B.C. Gates and W.O. Haag, J. Mol. Catal., 67 (1991) 363.
[8] J. Engelhardt and W.K. Hall, J. Catal., 125 (1990) 472.
[9] P.V. Shertukde, G. Marcelin, G.A. Sill and W.K. Hall, J. Catal., 136 (1992) 446.
[10] A. Corma, P.J. Miguel and A.V. Orchilles, J. Catal., 145 (1994) 171.
[11] G. Yaluris, J.E. Rekoske, L.M. Aparicio, R.J. Madon and J.A. Dumesic, J. Catal., 153 (1995) 54.
[12] G. Yaluris, J.E. Rekoske, L.M. Aparicio, R.J. Madon and J.A. Dumesic, J. Catal., 153 (1995) 65.
[13] H. Krannila, W.O. Haag and B.C. Gates, J. Catal., 135 (1992) 115.
[14] I.N. Senchenya and V.B. Kazansky, Catal. Lett., 8 (1991) 317.
[15] P. Viruela-Martin, C.M. Zicovich-Wilson and A. Corma, J. Phys. Chem., 97 (1993) 13713.
[16] G.J. Kramer, R.A. van Santen, C.A. Emeis and A.K. Nowak, Nature, 363 (1993) 529.
[17] V.B. Kazansky, I.N. Senchenya, M.V. Frash and R.A. van Santen, Catal. Lett., 27 (1994) 345.
[18] V.B. Kazansky, M.V. Frash and R.A. van Santen, Catal. Lett., 28 (1994) 211.
[19] S.R. Blaszkowski, A.P.J. Jansen, M.A.C. Nascimento and R.A. van Santen, J. Phys. Chem., 98 (1994) 12938.
[20] J.A. Lercher, R.A. van Santen and H. Vinek, Catal. Lett., 27 (1994) 91.
[21] S.J. Collins and P.J. O'Malley, J. Catal., 153 (1995) 94.
[22] M.J. Frisch, G.W. Trucks, M. Head-Gordon, P.M.W. Gill, M.W. Wong, J.B. Foresman, B.G. Johnson, H.B. Schlegel, M.A. Robb, E.S. Replogle, R. Gomperts, J.L. Andres, K. Raghavachari, J.S. Bincley, C. Gonzalez, R.L. Martin, D.J. Fox, D.J. Defrees, J. Baker, J.J.P. Stewart and J.A. Pople, GAUSSIAN 92, Revision A, Gaussian, Inc., Pittsburgh, PA, 1992.
[23] W.J. Henre, R. Ditchfield and J.A. Pople, J. Chem. Phys., 56 (1972) 2257.
[24] P.C. Hariharan and J.A. Pople, Theoret. Chim. Acta., 28 (1973) 213.
[25] M.S. Gordon, Chem. Phys. Lett., 76 (1980) 163.
[26] H.B. Schlegel, J. Comput. Chem., 6 (1982) 163.
[27] C. Gonzalez and H.B. Schlegel, J. Chem. Phys., 90 (1989) 2154.
[28] C. Moller and M.S. Plesset, Phys. Rev., 46 (1934) 618.
[29] C.M. Breneman and K.B. Wiberg, J. Comput. Chem., 11 (1990) 361.
[30] J. Engelhardt and W.K. Hall, J. Catal., 151 (1995) 1.
[31] L.R. Sierra, E. Kassab and E.M. Evleth, J. Phys. Chem., 97 (1993) 641.
[32] J.R. Hufton and R.P. Danner, AIChE J., 39 (1993) 954.
[33] M. Stockenhuber, F. Eder and J.A. Lercher, to be published.
[34] V.B. Kazansky, Accounts Chem. Res., 24 (1991) 379.
[35] V.B. Kazansky, Stud. Surf. Sci. Catal., 85 (1994) 251.
[36] M.T. Aronson, R.J. Gorte, W.E. Farneth and D. White, J. Am. Chem. Soc., 111 (1989) 840.
[37] J.F. Haw, B.R. Richardson, I.S. Oshiro, N.D. Lazo and J.A. Speed, J. Am. Chem. Soc., 111 (1989) 2052.
[38] R.A. van Santen and G.J. Kramer, Chem. Rev. 95 (3) (1995) 637.
[39] D.M. Brouwer and H. Hogeveen, Progr. Phys. Org. Chem., 9 (1972) 179.
[40] H. Hogeveen and A.F. Bickel, Chem. Commun., 13 (1967) 635.
[41] G.A. Olah, G. Klopman and R.H. Schlosberg, J. Am. Chem. Soc., 91 (1969) 3261.
[42] H. Hogeveen, C.J. Gaasbeek and A.F. Bickel, Rec. Trav. Chim., 88 (1969) 703.
[43] S. Brownstein and J. Bornais, Can. J. Chem., 49 (1971) 7.